Ultra high-resolution fluorescence excitation spectrum of $^1B_1$ pyrimidine in a molecular beam. Structural assignments, analysis of singlet–triplet perturbations, and implications for intersystem crossing in the isolated molecule

J. A. Konings, W. A. Majewski,[a] Y. Matsumoto,[b] D. W. Pratt,[a] W. Leo Meerts
Fysisch Laboratorium, K. U. Nijmegen, 6525 ED Nijmegen, The Netherlands

(Received 29 March 1988; accepted 2 May 1988)

We have observed, and assigned, the fluorescence excitation spectrum of the 0_0^0 band in the $^1B_1 \leftarrow {}^1A_1$ electronic transition of pyrimidine, at a resolution of ~ 10 MHz. The rotational constants of the $^1B_1$ state, the lowest excited singlet state, are $A' = 6352 \pm 3$, $B' = 5853 \pm 3$, and $C' = 3042.0 \pm 0.5$ MHz. The magnitudes of these constants are not very different from those of the ground ($^1A_1$) state. However, the in-plane **a** and **b** inertial axes in the $^1B_1$ state are rotated by 90° with respect to those of the $^1A_1$ state. The spectrum also exhibits numerous perturbations, evidenced by the presence of extra lines, anomalous intensities and lifetimes, and shifts of the main lines from their expected positions. The perturbations are strongly magnetic-field dependent, demonstrating that they arise from an intramolecular coupling of the $^1B_1$ state with nearly isoenergetic rovibronic levels of a lower triplet ($^3B_1$) state. Models are proposed to account for this behavior based on a deconvolution of the experimental spectrum and simulations of the observed Zeeman effects. The most satisfactory interpretation of the data (in the language of the zero-order states) is obtained if it is assumed that a single rovibronic $^1B_1$ level is spin–orbit coupled to one or a few $^3B_1$ levels, which in turn are coupled *via* rotationally dependent Coriolis interactions to a dense manifold of background levels, probably those of the $^1A_1$ state. Because the latter coupling is small, typically less than the linewidths in the spectra, it is manifested only in a K'_{+1} dependence of the lifetimes of selected molecular eigenstates and the reduced g values required to fit the magnetic-field dependence of their spectra.

I. INTRODUCTION

The past few years have witnessed enormous experimental and theoretical progress in the understanding of the electronic, vibrational, and rotational spectra of polyatomic molecules. For example, van der Meer *et al.*[1] have found that the *ultra* high-resolution fluorescence excitation spectrum of pyrazine (1,4-diazabenzene) contains many more lines than expected for an ordinary electronic transition between two zero-order singlet states. It is now known that these "extra" lines have their origin in an intramolecular coupling between levels of the upper singlet and nearly isoenergetic levels of a lower triplet state. Individual rotation–vibration levels of the ground electronic state of H_2CO with an excess vibrational energy of ~ 8000 cm^{-1} have been examined by Field, Kinsey, and co-workers.[2] At low values of the rotational quantum number J, the spectra are relatively simple but at higher values of J, the spectra rapidly become more complex. The observed level densities at $J = 10$ are several times larger than the known densities of vibrational levels. And Bordé *et al.*[3] have been able to resolve hyperfine and "superfine" splittings of less than one part in 10^{10} in the vibrational spectra of molecules like SF_6. The great surprise here is that the rotational substructure of these spectra at very high values of J is far simpler than had been anticipated.[4]

The key ingredient in these rather remarkable experiments is a high resolution laser operating in either the ultraviolet (UV), visible, or infrared region of the electromagnetic spectrum. In this paper we describe a further application of the tunable, single-frequency UV laser[5] to studies of the structural and dynamic properties of the first excited singlet state ($^1B_1$) of pyrimidine (1,3-diazabenzene) in the collision-free environment of a molecular beam. The (Doppler-limited) spectral resolution in these experiments is ~ 10 MHz, or about one part in 10^9, thereby permitting a complete rotational analysis of the 0_0^0 band in the $^1B_1 \leftarrow {}^1A_1$ fluorescence excitation spectrum. The results are interpreted in terms of a slightly perturbed, axis-switched, asymmetric rotor Hamiltonian, yielding the rotational constants of both the ground and excited electronic states.[6]

The $^1B_1$ state of pyrimidine is an example of an important class of problems where discrete rotation–vibration levels of a higher electronic state are imbedded in a higher density manifold of rotation–vibration levels belonging to one or more lower electronic states. Other examples recently studied by high resolution spectroscopy include CH_2,[7,8] SO_2,[9] glyoxal,[10] and benzene.[11] In the case of $^1B_1$ pyrimidine, the lower states of interest are the $^3B_1$ triplet state and the $^1A_1$ ground state. Initially prepared $^1B_1$ levels can therefore decay by two routes, intersystem crossing (ISC) and internal conversion (IC). Traditionally, studies of energy flow involving these states, either in the absence or presence of collisions, have been performed in the time domain.[12–16] Despite

[a] Present address: Department of Chemistry, University of Pittsburgh, Pittsburgh, PA 15260.
[b] Present address: Institute of Physical and Chemical Research (RIKEN), Wako, Saitama 351-01, Japan.

 0021-9606/88/161813-14$02.10

significant advances in our understanding of the decay behavior of the isolated (or collisionally perturbed) molecule, a characteristic of all of this work is a lack of knowledge about the nature of the zero-order levels involved in the state mixing that is a prerequisite for energy flow. These difficulties may be traced in most cases to the poorly defined coherence properties of pulsed light sources.

Ultra high-resolution spectroscopy with continuous-wave (cw) lasers provides an attractive alternative to the traditional approach to intramolecular dynamics, as illustrated for the aforementioned molecules by other workers[1–11] and for pyrimidine here. We find, in the case of pyrimidine, isolated perturbations in its fully resolved $^1B_1 \leftarrow {}^1A_1$ excitation spectrum that are magnetic-field dependent. The energy flow process that we are probing in the frequency domain is therefore ISC involving nearly isoenergetic rotation–vibration levels of the lowest triplet state. The "off-diagonal" terms that are responsible for producing these perturbations, and generating the mixed states necessary for energy flow, are identified using standard deconvolution schemes. A comparison of these results with lifetime measurements of selected single molecular eigenstates as a function of magnetic field then reveals that J_{J1} states are the most perturbed, demonstrating that rotations (perhaps via Coriolis coupling) play a significant role in the energy flow process. This then allows comment on the ISC process in the structurally similar pyrazine, where similar effects are observed but are not as easily analyzed since the density of perturbed states is much higher than in pyrimidine.[17]

II. EXPERIMENTAL

The experimental apparatus has been described in detail elsewhere.[18] Briefly, narrow band UV radiation was obtained by placing a $LiIO_3$ angle-tuned single crystal of 1 mm thickness in the focused arm of a modified Spectra Physics ring dye laser, generating about 1 mW of second harmonic power. Stabilized scans over 4 cm^{-1} with a laser linewidth of less than 0.5 MHz in the UV could easily be made. Absolute frequency calibration was accomplished using the absorption spectrum of iodine.[19] Relative laser frequencies were measured using a sealed-off, temperature-stabilized, Fabry–Perot interferometer, and were accurate to $\pm$ 1 MHz.

The molecular beam was formed by expanding a mixture of pyrimidine in argon through a 100 μm nozzle. In order to achieve rotational resolution the molecular beam was strongly collimated by a dual skimmer and differential pumping arrangement. This setup reduced the Doppler width to about 10 MHz. Power-normalized fluorescence excitation spectra were obtained by collecting the undispersed total fluorescence, detected by a EMI 9864/950 QA photomultiplier tube, and measured by a standard photon counting system. The experiment was interfaced to a PDP11-23/ + computer system.

Magnetic fields were generated by passing current ($\leqslant$5 A) through two coils in a non-Helmholtz configuration, and calibrated using a Hall probe. The accuracy is $\pm$ 5%. Lifetime measurements were performed using a single photon counting system. This system utilizes a pulse generator to modulate the cw laser and to start an Ortec 437A time-to-amplitude converter (TAC), which in turn is stopped by a signal from the photomultiplier tube. The TAC supplies an output pulse with a height proportional to the time elapsed between the start and stop, which serves as an input to a multichannel analyzer. An Ortec 463 constant fraction discriminator prevents the TAC from giving output if more than a single photon is detected in one cycle. Measured lifetimes are estimated to be accurate to $\pm$ 10%.

III. RESULTS AND INTERPRETATION

The 0_0^0 band of the $^1B_1 \leftarrow {}^1A_1$ electronic transition in pyrimidine has its origin at 31 072.658 cm^{-1}. Under the *ultra* high-resolution conditions employed in this work, the spectrum consists of a large number of transitions near the band origin (the Q branch) and clusters of lines separated by about 12 GHz going up (the R branch) and down (the P branch) in frequency from the central part of the spectrum, as shown in Fig. 1. These observations are in accord with the assignment of the 0_0^0 band as a c-type, parallel transition.[20] That pyrimidine is a near symmetric oblate top in both electronic states is also apparent from the small splittings of the different possible "$\Delta K_{+1} = 0$" transitions in each of the P- and R-branch clusters. If weak features are neglected, each of these clusters contains the expected number of lines, apart from accidental degeneracies, leading to the "zero-order" assignments shown in Fig. 1.

The regular pattern of lines described above is disturbed by two effects, both illustrated more clearly in the individual spectra shown in Figs. 2–4. One effect is that of axis switching.[21–23] Each P- and R-branch cluster (other than R 0 and P 1) consists of a closely spaced center group of lines, with $K_{+1} = 0$ and $K_{+1} \geqslant 2$, and two more widely spaced lines, with $K_{+1} = 1$. All of these lines are clearly resolved in Figs. 2–4. The separation of the outer pair of transitions depends on the $K_{+1} = 1$ level splittings in both electronic states which, for near oblate symmetric tops, are proportional to $(A - B)J(J+1)$.[24] An approximate value for this quantity in the ground state is known from earlier microwave work,[25] $(A'' - B'')$ being of order 200 MHz. Normal selection rules require that the splitting of the $K_{+1} = 1$ lines in the P and R branch be approximately equal to the difference in the $(A - B)J(J+1)$ values in the two states,[24] leading to the expectation that this splitting should be less than 400 and 1200 MHz in the R 1 and R 2 clusters, respectively. Figures 3 and 4 show that these splittings are about 1800 and 3700 MHz, respectively, much larger than expected. We conclude from this observation that the two in-plane inertial axes are switched on electronic excitation, leading to different selection rules. In particular, if we characterize a rotational level of the ground state by the quantum numbers $(J'', K''_{-1}, K''_{+1})$, and a level of the excited electronic state by the quantum numbers (J', K'_{-1}, K'_{+1}), then the selection rules for the axis-switched c-type transition are (e = even, o = odd); $(K''_{-1}, K''_{+1}) \leftrightarrow (K'_{-1}, K'_{+1}) = (ee) \leftrightarrow (oe)$, $(eo) \leftrightarrow (eo)$, $(oo) \leftrightarrow (oo)$, and $(oe) \leftrightarrow (ee)$.[23] Under these conditions, the splitting of the $K_{+1} = 1$ transitions is approximately equal to the *sum* of the $(A - B)J(J+1)$ values in the two states, thereby accounting for the larger splittings observed experi-

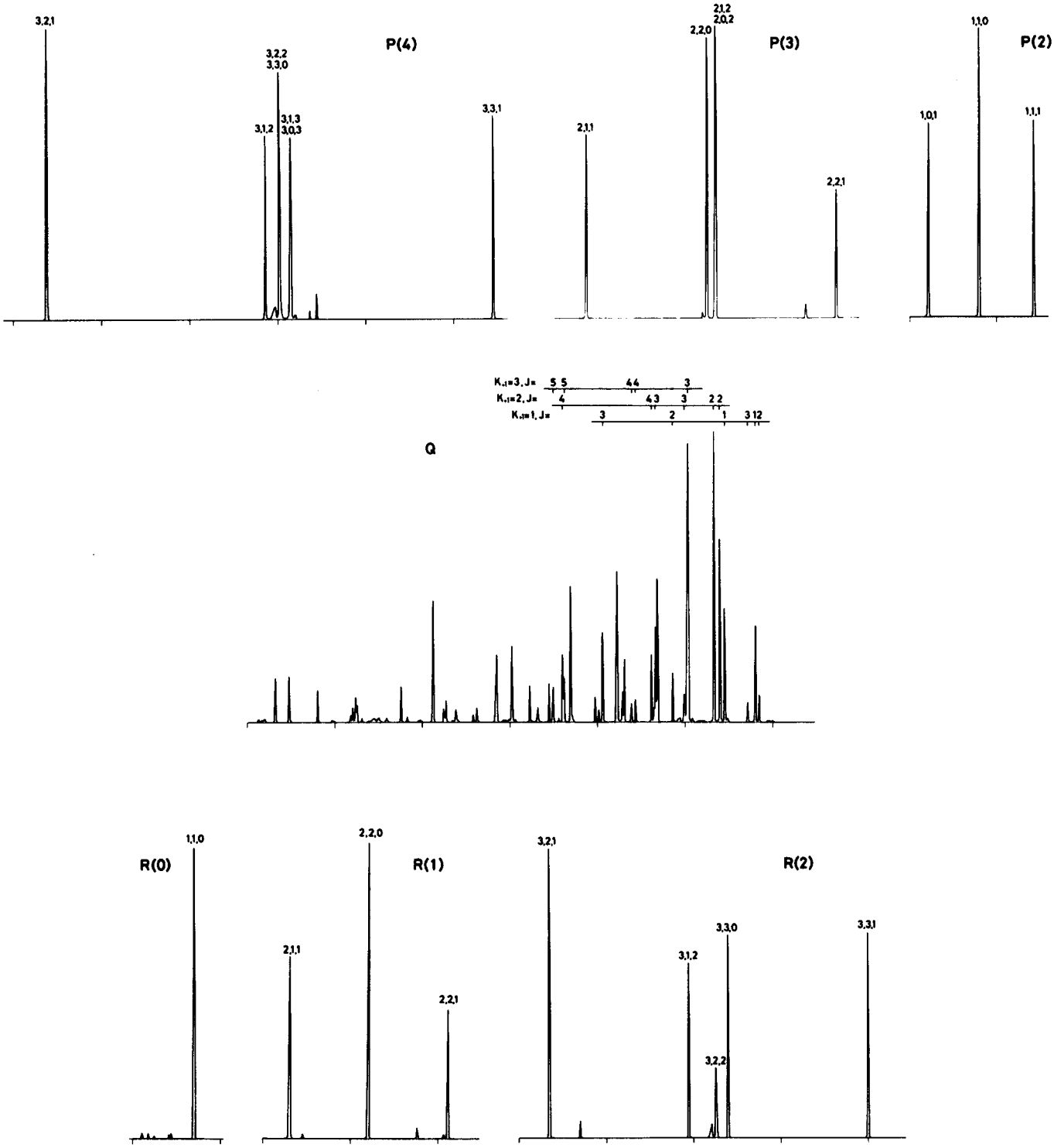

FIG. 1. Overview of the *ultra* high-resolution spectrum of the 0_0^0 band of the $S_1(^1B_1) \leftarrow S_0(^1A_1)$ electronic transition of pyrimidine in a molecular beam. The different branches ($P4$, $P3$, etc., where P, Q, R stand for $\Delta J = -1, 0, +1$ and the numbers refer to the J'' value of the lower state) are each separated by about 12 GHz. The relative intensities of the lines in each branch are individually scaled. Where shown, the quantum numbers denote the J', K'_{-1}, K'_{+1} values of the upper state levels. The frequency separation of each pair of markers is 1 GHz. Frequency increases from left to right, and top to bottom.

mentally. An overall fit of the spectrum confirmed this explanation.

The second irregular feature in the *ultra* high-resolution spectrum is that there are perturbations, evidenced particularly by anomalous intensities of some of the main lines and the presence of extra lines. The planar pyrimidine molecule, being rigid, can be characterized in the C_{2v} molecular symmetry group. The molecule has two pairs of equivalent atoms; the two nitrogen atoms and two of the four hydrogens. As a consequence of the Pauli exclusion principle, dif-

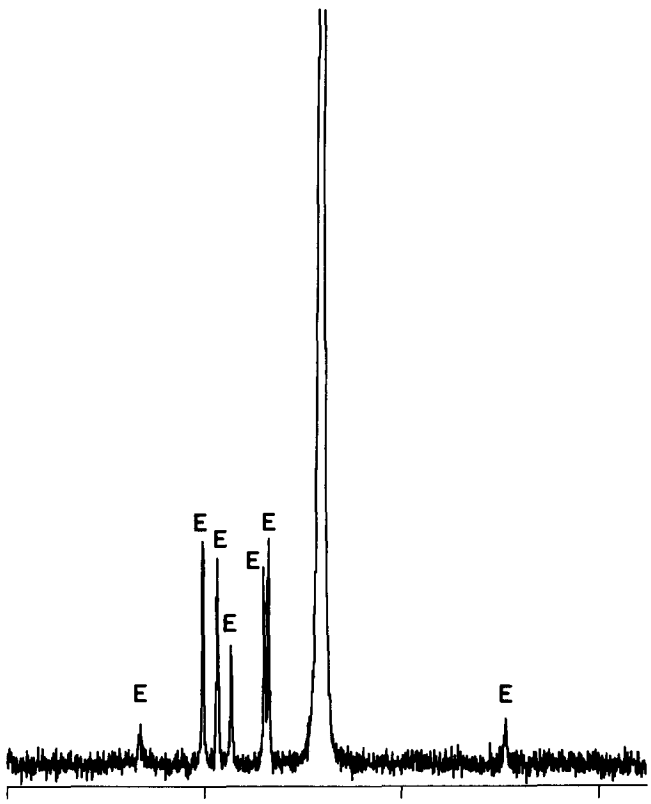

FIG. 2. The $R0$ ($J' = 1$) branch. "E" denotes extra lines observed at high gain, numbered sequentially from left to right. The separation of each pair of markers is 1 GHz. Frequency increases from left to right.

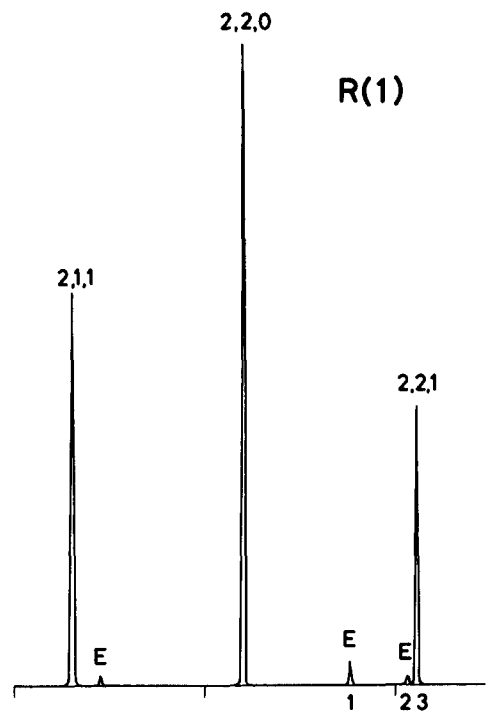

FIG. 3. The $R1$ ($J' = 2$) branch. Quantum numbers denote the J',K'_{-1},K'_{+1} values of the upper state levels. "E" denotes extra lines, numbered sequentially from left to right. The separation of each pair of markers is 1 GHz. Frequency increases from left to right.

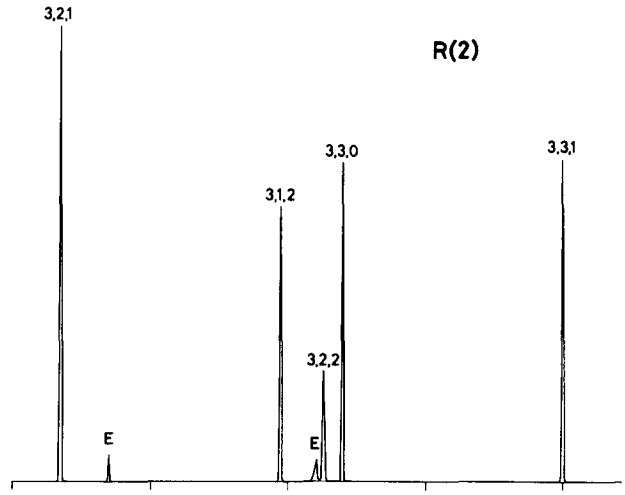

FIG. 4. The $R2$ ($J' = 3$) branch. Quantum numbers denote the J',K'_{-1},K'_{+1} values of the upper state levels. "E" denotes extra lines, numbered sequentially from left to right. The separation of each pair of markers is 1 GHz. Frequency increases from left to right.

ferent rotational levels have different nuclear spin statistical weights, $g_n = 15$ for the $(K''_{-1},K''_{+1}) = (ee)$ or (oo) levels and $g_n = 21$ for the (eo) or (oe) levels.[26] Differences in level populations and Hönl–London factors notwithstanding (both are relatively small in this case), we expect therefore intensity ratios of 21/15 for transitions originating in (eo) [or (oe)] levels compared to those originating in (ee) [or (oo)] levels. Much larger differences are observed experimentally. For example, the R 1 transition originating in (J'', K''_{-1}, K''_{+1}) = (1,0,1) [and terminating in J', K'_{-1}, K'_{+1}) = *(2,2,1)*] is weaker than the R 1 transition originating in (1,1,1) [and terminating in (2,1,1)] (cf. Fig. 3), whereas this ratio should be 21/15. Other perturbed lines displaying irregular intensities include $(3,2,1) \rightarrow (2,2,1)$, $(2,1,1) \rightarrow (1,1,1)$, $(2,2,1) \rightarrow (1,0,1)$, $(2,1,2) \rightarrow (3,2,2)$; and several overlapped pairs of lines [$(4,4,0) \rightarrow (3,3,0)$ and $(4,3,2) \rightarrow (3,2,2)$, $(4,1,3) \rightarrow (3,1,3)$ and $(4,2,3) \rightarrow (3,0,3)$, and $(3,2,2) \rightarrow (2,1,2)$ and $(3,1,2) \rightarrow (2,0,2)$], for which the individual intensities are more difficult to determine. Here, italic quantum numbers refer to upper state levels that are accessed via both P- and R-branch transitions and are observed to be perturbed in both cases. All other perturbed levels can be accessed via only one of the two branches, but not both.

Intensity anomalies were also observed in the Q branch, not only for transitions terminating in the levels noted above, but also for several additional levels with $K'_{+1} = 2$ and 3. This is illustrated in Fig. 5 which compares the measured relative peak heights (all lines have approximately the same width) with relative intensities calculated according to the factor

$$I = I_0 g_n \frac{(K''_{+1})^2}{J''(J''+1)} (2J''+1) e^{-E(J'',K''_{+1})/kT}. \quad (1)$$

Transitions terminating in the levels (3,2,2), (3,0,3) and (3,1,3) (an overlapped pair), (4,2,3), and (4,1,3) are much weaker than predicted on the basis of Eq. (1). In addition, some levels appear to have more oscillator strength than expected [e.g., (4,3,2)].

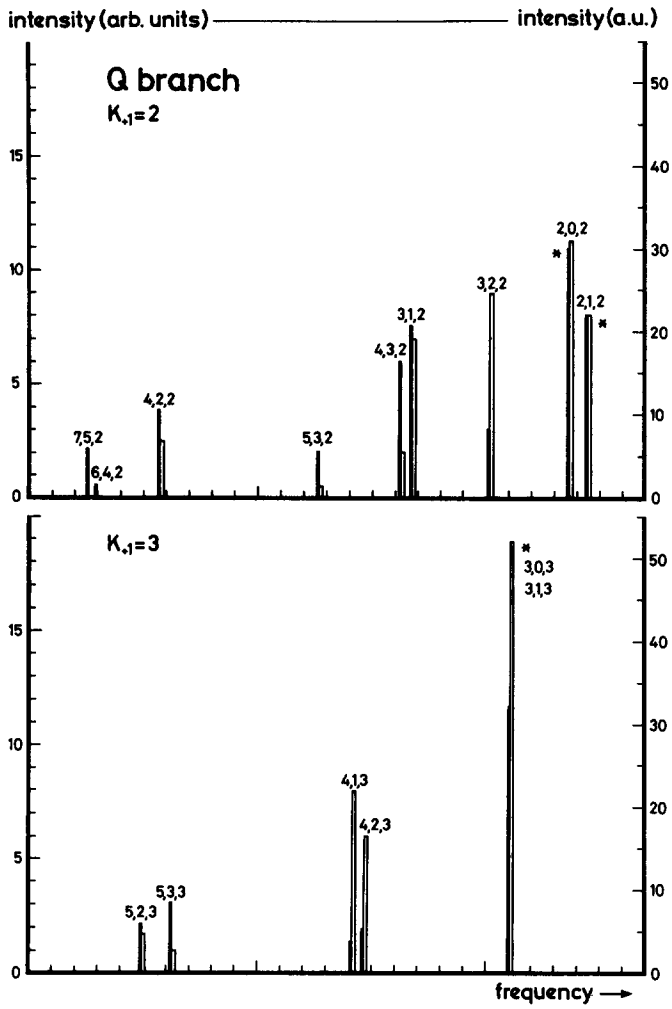

FIG. 5. Calculated (open bars) and measured (solid bars) intensities of the assigned $K'_{+1} = 2$ and $K'_{+1} = 3$ transitions in the Q branch. Those transitions denoted by asterisks are scaled according to the vertical axis on the right, all other transitions are scaled according to the vertical axis on the left. The separation of each pair of markers is 100 MHz.

Finally, there also appear in the immediate vicinity of some of these perturbed lines extra lines, much as in the case of CN[27] and other well-known examples of perturbations in the spectra of diatomic molecules.[28] Several examples are shown in Figs. 2–4. The R 0 transition (0,0,0) → (1,1,0) has at least seven extra lines in its vicinity, the R 1 transition has at least three extra lines [two in the (2,2,1) cluster], and the R 2 transition has at least five extra lines [three in the (3,2,2) cluster and one in the (3,3,0) cluster]. As the latter two transitions were only recorded at low gain, it is likely that still more extra lines would be observed at higher gain. Many other extra lines also appear in the P- and Q-branch spectra.

More information about the nature of these perturbations was provided by magnetic field measurements. For example, Fig. 6 compares the R 1 spectrum at zero field and at a field of 32 G. Whereas the two unperturbed lines (and two of the extra lines) are relatively unaffected by the application of this weak field, both the perturbed and extra lines associated with the transition (1,0,1) → (2,2,1) are strongly affected. Still higher fields (up to 66 G) quench the first extra line, split the second, and produce further splittings of the "(1,0,1) → (2,2,1)" line.

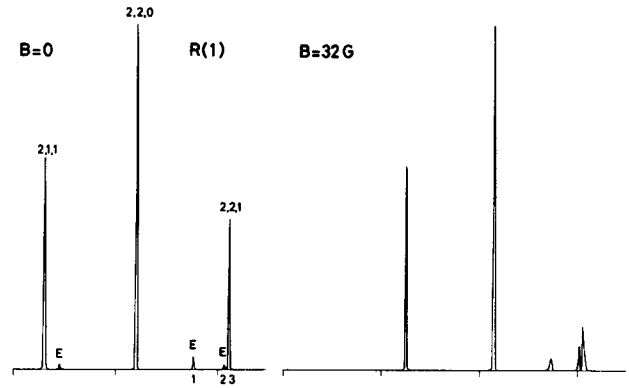

FIG. 6. The R 1 branch, in zero magnetic field (left) and at a field of 32 G (right). The separation of each pair of markers is 1 GHz. Frequency increases from left to right.

Measurements of the lifetimes of several of the levels accessed in the *ultra* high-resolution spectrum were also made, the results of which are summarized in Table I. An example is provided by the data for two lines in the R 1 transition. Both of the levels (2,2,0) and (2,2,1) decay exponentially, but the latter (a perturbed level) has a much longer lifetime than the former (742 vs 483 ± 27 ns). The lifetimes

TABLE I. Measured fluorescence lifetimes of selected levels in the *ultra* high-resolution spectrum of pyrimidine.

Transition	(J',K'_{-1},K'_{+1})	Lifetime, ns	Estimated error, ns	Notes
$P4$	(3,2,1)	650	15	w[a]
	(3,1,2)	773	40	w
	(3,3,0)			
	(3,2,2)	817	61	m
	(3,1,3)			
	(3,0,3)	812	26	i
	(3,3,1)	662	25	w
$P3$	(2,1,1)	558	10	i
	(2,2,0)	586	20	i
	(2,1,2)			
	(2,0,2)	550	42	···
	(2,2,1)	832	120	s
$P2$	(1,0,1)	731	82	w
	(1,1,0)	571	15	i
	(1,1,1)	710	40	s
$P1$	(0,0,0)	557	30	···
$R0$	(1,1,0)	547	30	···
$R1$	(2,1,1)	560	16	i
	(2,2,0)	483	27	i
	(2,2,1)	742	27	s
$R2$	(3,2,1)	682	16	w
	(3,1,2)	745	33	w
	(3,2,2)	890	50	m
	(3,3,0)	667	50	m
	(3,3,1)	693	11	w

[a] Denotes whether decay is sensitive (s = strong, m = medium, w = weak) or insensitive (i) to magnetic fields.

TABLE II. Molecular constants of pyrimidine in its ground ($^1A_1$) and first excited singlet ($^1B_1$) states. ΔI ($= I_c - I_b - I_a$) is the inertial defect.

State	Constant	Value
$^1A_1$	A'' [a]	6276.80 (4) MHz
	B'' [a]	6067.12 (4) MHz
	C'' [a]	3084.47 (4) MHz
	$\Delta I''$ [a]	0.0328 amu Å^2
$^1B_1$	A' [b]	6352 (3) MHz
	B' [b]	5853 (3) MHz
	C'	3042.0 (5) MHz
	$\Delta I'$	0.240 amu Å^2
	$\nu_0 = 31\,072.658$ (5) cm^{-1}	

[a] Reference 25.

[b] The orientations of the a and b inertial axes are switched on electronic excitation. See the text.

of higher K'_{+1} levels are typically longer than those for lower K'_{+1} levels. Note, also, that where a specific level can be reached either via a *P*- or an *R*-branch transition, the lifetimes measured in the two experiments are in good agreement with each other.

We conclude from all of these observations, then, that the perturbing state in $^1B_1$ pyrimidine is triplet in character, probably $^3B_1$.

Given the existence of these irregularities in the spectrum, we used the following procedure to determine the rotational constants of $^1B_1$ pyrimidine. First, the normal selection rules were used to identify all strong transitions in the *P* and *R* branches, and the positions of these lines were fit to the asymmetric rotor Hamiltonian of Watson,[29] using the previously derived values of the ground state rotational constants[25] and the modified selection rules to account for axis switching. The excited state constants derived from this fit were then used to analyze the *Q*-branch line positions. Quite a good correspondence was found between theory and experiment for 20 lines up to about 2500 MHz from the *Q*-branch origin, except for lines terminating in $K'_{+1} = 1$. We then ignored these lines, as well as other *P*- and *R*-branch transitions terminating in $(J', K'_{-1}, K'_{+1}) = (0,0,0)$, $(1,1,1)$, and $(2,2,1)$, to obtain refined values of the constants of both states in a final fit of all of the remaining data. Line intensities were not used, quantitatively, in this analysis. The derived values of the inertial parameters for both $^1A_1$ and $^1B_1$ pyrimidine are given in Table II. The values shown for the $^1A_1$ state are those from the more accurate microwave study[25]; our values are in good agreement with them.

The largest changes in the moments of inertia that occur on electronic excitation involve motion about the two in-plane axes. The long-axis rotational constant increases by 285 MHz, whereas the short-axis rotational constant decreases by 425 MHz, leading to the observed axis switching. Clearly, then, excitation of a nitrogen lone-pair electron into a π^* orbital results in a contraction of the molecule along the short axis and expansion of the molecule along the long axis. There must also be a slight increase in the size of the ring since *C* also decreases.

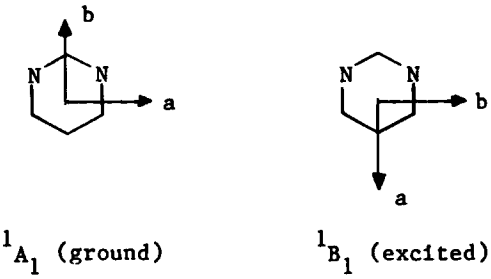

These changes are consistent with the expected form of the highest occupied and lowest occupied molecular orbitals of pyrimidine[30] and with the vibrational activity in its absorption[20] and fluorescence[31] spectra.

Returning now to the subject of perturbations, which will be the main focus of this paper, we compare in Table III the observed frequencies of all assigned *P*-, *Q*-, and *R*-branch transitions with those calculated using the parameters in Table II, all frequencies being referred to the band origin. We also give estimates of the experimental precision of each line position. Most lines can be fit to this precision; the standard deviation of the fit is $\pm$ 20 MHz. But the observed frequencies of several of the lines are shifted from the theoretical values by as much as 140 MHz. These are not large differences, but they are clearly outside of experimental error at this level of resolution. The most shifted levels are those with $J' = K'_{-1}$, $K'_{+1} = 1$. The level with $(J', K'_{-1}, K'_{+1}) = (2,2,1)$ is the most striking. Its energy differs from the calculated values by 123, 117, and 135 MHz in the *P*-, *Q*-, and *R*-branch transitions terminating in this level. Other strongly affected levels are (0,0,0) and (1,1,1). Moreover, the most shifted levels are also those that exhibit (where examined) unusual intensities and a strong magnetic sensitivity. This shows that the perturbing triplet levels are also responsible for the observed frequency shifts, as well as for the existence of extra lines. Thus, an analysis of these effects should provide important information about the interactions responsible for ISC in the isolated molecule.

IV. PERTURBATION ANALYSIS

A. Deconvolution of the spectra

An important first step in this analysis is the deconvolution, or deperturbation, of the spectrum into a set of zero-order states and coupling matrix elements. Typically, we find in the spectrum isolated perturbations; i.e., only one main line in a given *P*- or *R*-branch cluster is perturbed. All other main lines appear to be relatively unperturbed, at least at low J'. However, we also find in the vicinity of the perturbed line more than one extra line, suggesting that more than one zero-order triplet level is (directly or indirectly) coupled to the zero-order singlet level. Therefore, a 2×2 analysis of the problem will not suffice. Instead, we adopt the deconvolution procedure of Lawrance and Knight,[32] in which it is assumed that only one of the component states (the zero-order singlet level $|S^0\rangle$) of the perturbed manifold carries oscillator strength, and that this state is mixed with one or more dark states (the zero-order triplet levels $|T_i^0\rangle$) in its vicinity. The dark states are further assumed in this

TABLE III. Observed and calculated rovibronic frequencies in the 0_0^0 band of the $^1B_1 \leftarrow {}^1A_1$ transition of pyrimidine. Frequencies are in MHz relative to the band origin ν_0. Lines marked with an asterisk were omitted from the least-squares fit (see the text).

Transition	(J',K'_{-1},K'_{+1})	Observed value, MHz	Estimated error, MHz	Observed − calc., MHz
$P4$	(3,2,1)	− 52 788	40	− 67
	(3,1,2)	− 50 284	40	− 38
	(3,3,0)			− 64
	(3,2,2)	− 50 126	50	− 20
	(3,1,3)			
	(3,0,3)	− 49 996	40	− 20
	(3,3,1)	− 47 677	40	− 55
$P3$	(2,1,1)	− 38 794	40	9
	(2,2,0)	− 37 417	40	21
	(2,1,2)			
	(2,0,2)	− 37 322	40	25
	(2,2,1)	− 35 924*	40	123
$P2$	(1,0,1)	− 25 367	40	− 4
	(1,1,0)	− 24 776	40	60
	(1,1,1)	− 24 137*	40	97
$P1$	(0,0,0)	− 12 231*	40	112
Q	(6,3,4)			
	(6,2,4)	− 2 822	20	− 24
	(6,2,5)			
	(6,1,5)	− 2 379	20	30
	(5,2,3)	− 2 209	20	− 11
	(4,2,2)	− 2 096	20	− 2
	(5,3,3)	− 2 084	20	− 4
	(6,1,6)			
	(6,0,6)	− 2 002	20	− 3
	(5,1,5)			
	(5,0,5)	− 1 465	20	− 11
	(4,1,3)	− 1 305	20	− 14
	(4,2,3)	− 1 256	20	1
	(4,3,2)	− 1 071	20	5
	(3,1,2)	− 1 021	20	− 1
	(4,1,4)			
	(4,0,4)	− 999	20	− 4
	(2,1,1)	− 821	20	1
	(3,2,2)	− 692	20	24
	(3,1,3)			
	(3,0,3)	− 647	20	− 26
	(2,0,2)	− 350	20	18
	(2,1,2)	− 280	20	17
	(1,0,1)	− 223	20	34
	(3,3,1)	40	20	− 60
	(1,1,1)	122*	20	88
	(2,2,1)	165*	20	117
$R0$	(1,1,0)	12 286	40	80
$R1$	(2,1,1)	23 462	40	16
	(2,2,0)	24 366	40	31
	(2,2,1)	25 290*	40	135
$R2$	(3,2,1)	34 446	40	− 11
	(3,1,2)	36 047	40	25
	(3,2,2)	36 362	40	51
	(3,3,0)	36 501	40	9
	(3,3,1)	38 103	40	22

procedure to be prediagonalized with respect to other possible intramolecular couplings; i.e., there are no off-diagonal terms connecting the $|T_i^0\rangle$. Thus, in this basis the Hamiltonian takes the form

$$\hat{H}_0 = \begin{vmatrix} \epsilon_S^0 & v_1 & v_2 & \cdot & \cdot & v_i \\ v_1 & \epsilon_{T_1}^0 & 0 & 0 & \cdot & 0 \\ v_2 & 0 & \epsilon_{T_2}^0 & \cdot & \cdot & \cdot \\ \cdot & 0 & \cdot & \cdot & \cdot & \cdot \\ \cdot & \cdot & \cdot & \cdot & \cdot & \cdot \\ v_i & 0 & \cdot & \cdot & \cdot & \epsilon_{T_i}^0 \end{vmatrix}, \tag{2}$$

where ϵ_S^0, $\epsilon_{T_1}^0$, $\epsilon_{T_2}^0$,...,$\epsilon_{T_i}^0$ are the zero-order energies and $v_i = \langle S^0|\hat{H}_{ST}|T_i^0\rangle$. If $|\mathrm{ME}_j\rangle$ denotes a molecular eigenstate, it can be expanded according to

$$|\mathrm{ME}_j\rangle = c_S|S^0\rangle + \sum_i c_{T_i}|T_i^0\rangle \tag{3}$$

and has the energy

$$\epsilon_{\mathrm{ME}_j} = \epsilon_S^0 + \sum_i \frac{\langle S^0|\hat{H}_{ST}|T_i^0\rangle}{\epsilon_{T_i}^0 - \epsilon_S^0}\epsilon_{T_i}^0 . \tag{4}$$

Since the coupled states have different multiplicities, it is clear that the interaction responsible for this mixing process ($\hat{H}_{ST}$) must be spin–orbit in nature, at least in part.

What are required in the approach of Lawrance and Knight[32] are the energies of the molecular eigenstates (ϵ_{ME_j}) and their singlet characters, c_{S_j}. Both types of information can be determined from the spectra, from the relative positions of the lines and their absorption intensities. (From our spectra only the excitation intensities can be determined. It will later be shown that these are equal to the absorption intensities only if the lifetimes of the dark states can be neglected.) The absorption intensities are normalized to unity, to give the c_{S_j} values, and the energies ϵ_{ME_j} are referred to the energy of the zero-order singlet, determined by the "center-of-gravity" method:

$$\epsilon_S^0 = \sum_j |c_{S_j}|^2 \epsilon_{\mathrm{ME}_j} . \tag{5}$$

Then, the energies of the zero-order triplet levels ($\epsilon_{T_i}^0$) may be calculated from the peak positions in the function $B(E)$,

$$B(E) = \frac{\mathrm{Im}\, G_{SS}(E)}{[\mathrm{Re}\, G_{SS}(E)]^2 + [\mathrm{Im}\, G_{SS}(E)]^2}, \tag{6}$$

where the real (Re) and imaginary (Im) parts of the Green's function $G_{SS}(E)$ are defined as

$$\mathrm{Re}\, G_{SS}(E) = \sum_j |c_{S_j}|^2 \frac{\epsilon_{\mathrm{ME}_j} - E}{(\epsilon_{\mathrm{ME}_j} - E)^2 + \Gamma_{\mathrm{ME}_j}^2} \tag{7}$$

and

$$\mathrm{Im}\, G_{SS}(E) = \sum_j |c_{S_j}|^2 \frac{\Gamma_{\mathrm{ME}_j}}{(\epsilon_{\mathrm{ME}_j} - E)^2 + \Gamma_{\mathrm{ME}_j}^2} \tag{8}$$

giving a "spectrum" of $B(E)$ values. Finally, the matrix elements are calculated by multiplying the peak intensities in $B(E)$ by the corresponding linewidths Γ_{ME_j}. In agreement with earlier work,[32] we find that the derived values of both $\epsilon_{T_i}^0$ and v_i are relatively insensitive to the choice of Γ_{ME_j}, over the range 0.1–10 MHz.

The results of our calculations are given in Table IV. Listed there are the values of ϵ_{ME_j} and $|c_{S_j}|^2$, determined

TABLE IV. Energies and intensities of the perturbed $R\,0$, $R\,1$, and $R\,2$ molecular eigenstates of the zero-point vibrational level of $^1B_1$ pyrimidine, together with the relative energies and coupling matrix elements of the interacting zero-order $^3B_1$ levels.[a]

ME		ϵ_{ME_j}, MHz[b]	$\lvert c_{S_j}\rvert^2$, arb.	$\epsilon^0_{T_i}$, MHz[c]	v_i, MHz
$R\,0$	1	−897	33	−895	42
(1,1,0)	2	−580	168	−574	57
	3	−504	156	−498	55
	4	−438	90	−435	40
	5	−269	151	−266	27
	6	−247	170	−243	35
	7	22	13 800	(0)	···
	8	958	31	956	44
$R\,1$	1	−321	5	−294	93
(2,2,1)	2	−21	2	−19	9
	3	29	58	(0)	···
$R\,2$	1	−56	7	−53	11
(3,2,2)	2	−42	11	−34	20
	3	7	54	(0)	···
	4	20	20	17	6
R2	5	−55	3	−47	22
(3,3,0)	6	9	157	(0)	···

[a] ME's are numbered in order of increasing frequency, as shown in Figs. 2–4.
[b] Determined by the center-of-gravity method (see the text).
[c] Relative to the energy of $|S^0\rangle$.

from the spectra, and of $\epsilon^0_{T_i}$ and v_i, determined from applying the deconvolution procedure to four clusters of lines; the eight (1,1,0) ME's, the three (2,2,1) ME's, the four (3,2,2) ME's, and the two (3,3,0) ME's, the latter two clusters having been treated independently. Several facts are immediately apparent on examination of these results. The first, and most important, is that the magnitudes of the spin–orbit matrix elements are small. The larger couplings tend to involve zero-order triplets that are further displaced from the singlet "origin," but in no case do these matrix elements exceed 100 MHz. A direct consequence of this result is that the oscillator strength is distributed over a very narrow range of energy, ~2 GHz in the case of the $R\,0$ "line," and less in the case of the other lines. The displacements of the ME's from their zero-order positions are also small. For example, the zero-order singlet level is shifted by values of only 22, 29, 7, and 9 MHz in the four clusters. These shifts are typically smaller than those deduced from a comparison of the observed and calculated line positions in the experimental spectrum (cf. Table III).

The ME's also retain much of their zero-order identity. One measure of this limited degree of mixing is the set of eigenvectors in the zero-order basis. For example, the strongest line in the $R\,0$ cluster can be described as

$$\begin{aligned}|\mathrm{ME}_7\rangle &= c_{S_7}|S^0\rangle + \sum_i c_{T_i}|T_i\rangle \\ &= 0.972|S^0\rangle + 0.044|T^0_1\rangle + 0.094|T^0_2\rangle \\ &\quad + 0.102|T^0_3\rangle + 0.085|T^0_4\rangle + 0.089|T^0_5\rangle \\ &\quad + 0.127|T^0_6\rangle - 0.046|T^0_7\rangle . \end{aligned} \tag{9a}$$

Thus, all seven zero-order triplet levels make comparable contributions to the character of this eigenstate, but the cumulative triplet contribution is small (~5%). Similar conclusions can be made regarding the remaining ME's, at least at zero magnetic field. However, there is a trend towards larger S^0–T^0_i mixing as J' and K' increase; the corresponding strongest lines in the (2,2,1) and (3,2,2) clusters are

$$|\mathrm{ME}_3\rangle \equiv 0.945|S^0\rangle + 0.271|T^0_1\rangle + 0.185|T^0_2\rangle , \tag{9b}$$

$$\begin{aligned}|\mathrm{ME}'_3\rangle &= 0.766|S^0\rangle + 0.139|T^0_1\rangle + 0.377|T^0_2\rangle \\ &\quad - 0.502|T^0_3\rangle , \end{aligned} \tag{9c}$$

respectively, with cumulative triplet contributions of 11% and 41%. These are still small. Thus, to a good approximation, it is still possible to speak (at low J',K') of "singlet" and "triplet" states at energies near the zero-point vibrational level of $^1B_1$ pyrimidine.

B. The Zeeman effect

More information about the character of these states, and about the mechanisms that are responsible for mixing them, can be determined from their behavior in the presence of a magnetic field, just as in the case of the related problem in pyrazine.[33] A triplet state can be represented as $|T\rangle = |\{v\}NKSJM_J\rangle$ in the Hund's case (b) limit, where **N** is the angular momentum due to the pure rotational motion of the molecular frame and K ($\sim K_{+1}$ for pyrimidine) is its projection on the top axis, **S** is the electron spin angular momentum, $\mathbf{J} = \mathbf{N} + \mathbf{S}$ is the total angular momentum, and M_J is its projection on a space-fixed axis. The symbol $\{v\}$ stands for all of the vibronic quantum numbers. In pyrimidine, the rotational level structure is mainly governed by N, with level spacings of order $N \times 20$ GHz. Spin–spin, spin–orbit, and spin–rotational couplings split each rotational level into a set of three levels, $J = N + 1$, $J = N$, and $J = N - 1$ (Fig. 7). Typically, this fine structure splitting is small (~1 GHz)[34] compared to the rotational level spacing, and J is a good quantum number in zero external field.

Each triplet level is $2J + 1$ degenerate. This M_J degeneracy is removed by the application of an external field. The first-order energy shift is given by

$$\langle T|\hat{H}_Z|T\rangle = \mu_B B g M_J , \tag{10}$$

where μ_B is the Bohr magneton, B is the magnetic field strength, and g is the g factor, given by

$$g = 2.002\left[\frac{J(J+1) + S(S+1) - N(N+1)}{2J(J+1)}\right] . \tag{11}$$

Here, we consider only the diagonal, isotropic component of the electron spin Zeeman operator, off-diagonal electron spin, and rotational Zeeman terms being unimportant at the low field strengths and N values employed in this work. Unfortunately, our experiments give no information about the $\{v\}$ or N values of the coupled triplet levels, except that N is restricted (since J is conserved) to $N = J, J \pm 1$. So we used a trial-and-error method to simulate the observed Zeeman effects. By assuming values of N for each affected level, the g factors could be defined, and the first-order energy shifts computed according to Eq. (10). The influence of a field on

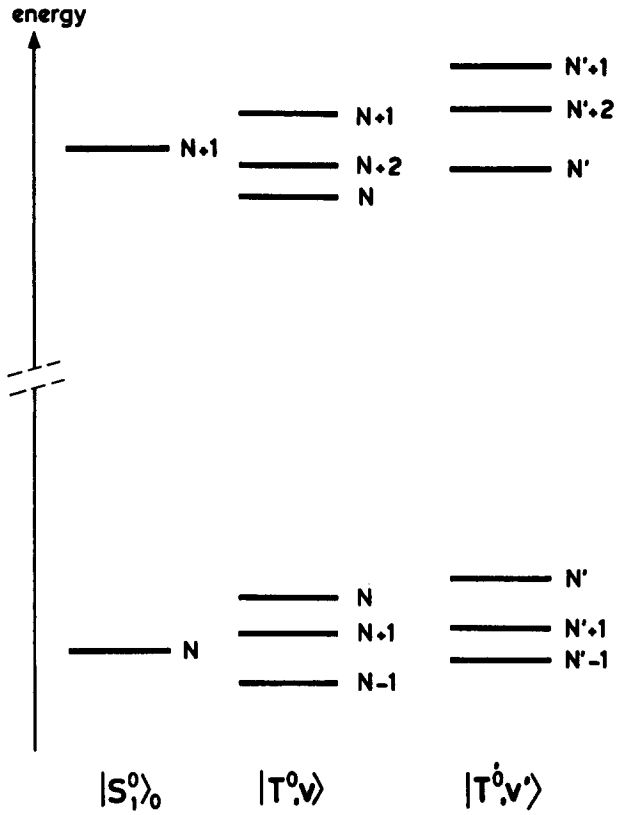

FIG. 7. Rotational level structure of the zero-order states $|S^0,0\rangle$, $|T^0,v\rangle$, and $|T^0,v'\rangle$, v and v' being two of the many different possible vibrational levels of $|T^0\rangle$. Each level is labeled by J, the total angular momentum quantum number. In pyrimidine, each $|S^0,0,N\rangle$ level interacts only with those triplet levels lying within $\pm$ 1 GHz of the origin. Singlet–triplet coupling is allowed only between those zero-order states having the same value of J.

the energies of the ME's could then be determined simply by adding the Zeeman contributions from Eq. (10) to the Hamiltonian of Eq. (2), defined for each cluster of lines by the deconvolution results (Table IV), in the basis of zero-order states. Diagonalization then gives the energies of the ME's as a function of field and the corresponding eigenvectors, each of which contains a term $|c_S|^2$ that is proportional to the absorption intensity. Multiplying this term by the transition dipole moment[36] then yields spectral intensities that may be compared with experiment, to determine whether correct assumptions for the N values of the triplet levels have been made. In practice, this trial-and-error method can be used if only a small number of dark states is involved. This is clearly the case for the rovibronic spectrum of pyrimidine.

As a partial test of our procedures, we first calculated the effective g factor associated with the R 0 line. Of course, if the upper state accessed in this transition were a pure singlet state, it would exhibit no magnetic sensitivity at all. But, as was shown in the recent work of Ohta *et al.*,[37] the fluorescence decay of R 0 following nanosecond laser excitation exhibits field dependent quantum beats that were attributed to weak singlet–triplet mixing. The observation of weak "extra" lines in the R 0 cluster (Fig. 2) confirms this interpretation. Ohta *et al.*[37] also estimated a g factor of 0.02 from the field dependence of the beat frequency, assumed to correspond to the energy separation of two Zeeman sublevels with $M_J = \pm 1$. Such a small g factor should produce little or no shift of the spectral lines at low fields. In agreement with this, we find no shifts of any of the lines in Fig. 2 up to an applied field of 66 G, even at $\sim$10 MHz resolution. But we can estimate the g factor from our data by assuming that the magnetic sensitivity is associated with the small triplet character of the brightest eigenstate in the R 0 spectrum, $|\mathrm{ME}_7\rangle$ [Eq. (9a)]. The isotropic part of the electronic Zeeman operator acting on this state yields

$$\begin{aligned}\langle \mathrm{ME}_7|\hat{H}_Z|\mathrm{ME}_7\rangle &= \sum_{T,T'} c_T^* c_{T'} \langle T|\hat{H}_Z|T'\rangle \\ &= \sum_T |c_T|^2 \langle T|\hat{H}_Z|T\rangle \\ &= \sum_T |c_T|^2 g_T M_{J_T} \mu_B B . \end{aligned} \tag{12}$$

Here we have used the facts that $\hat{H}_Z$ acts only on triplet states and is diagonal in $|T\rangle$. Since $J_T = 1$, N_T may be 0, 1, or 2, with g values of $g_T = 2$, 1, and -1, respectively. Taking $N_T = 0$ for all coupled triplets gives an upper limit to the "effective" g factor of

$$g^{\mathrm{eff}} = \left(\sum_T |c_T|^2 g_T M_{J_T}\right)_{\max} = 0.11 . \tag{13}$$

Clearly, g^{eff} may be less than this since there is no *a priori* reason to take all $N_T = 0$. A mixing *between* triplet states could further reduce the g factor (*vide infra*). Thus, the two sets of experiments appear to be in reasonable agreement.

A more stringent test of our procedures is provided by a comparison of theory and experiment for the remaining clusters. The results for the perturbed (2,2,1) cluster are shown in Fig. 8. Experimentally [Fig. 8(a)], it is observed that this portion of the R 1 transition is markedly affected by the application of small fields; both the strong "singlet" line (3) and the two weak "triplet" lines (1 and 2) shift and split into several components even at fields as low as 15 G. This behavior is qualitatively reproduced by the calculated spectra, shown in Fig. 8(b). Here, we find that the best agreement between theory and experiment is obtained by assuming $N_1 = 1$ and $N_2 = 3$. (Since the upper state J is 2 for the R 1 transition, the possible values of N are 1, 2, and 3.) At zero field, the calculated spectrum (not shown) is of course identical with the experimental one. But the quantitative agreement deteriorates progressively with the application of a field. The most striking discrepancy is that line 2 gains

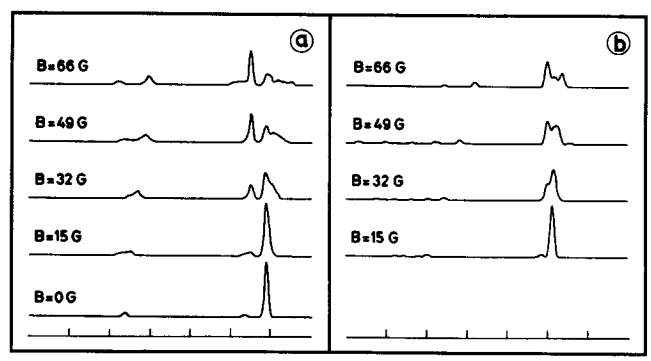

FIG. 8. Comparison of observed (left) and calculated (right) magnetic field dependence of the perturbed (2,2,1) cluster in the R 1 transition. The separation of each pair of markers is 100 MHz. The frequency increases from left to right.

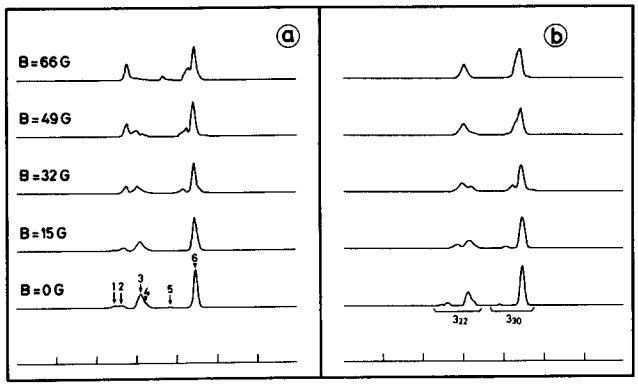

FIG. 9. Comparison of the observed (left) and calculated (right) magnetic field dependence of the perturbed (3,2,2) and (3,3,0) clusters in the R 2 transition. The separation of each pair of markers is 100 MHz. The frequency increases from left to right.

significant intensity at the expense of line 3 experimentally, even at very low fields, but not theoretically. The calculated Zeeman splitting is also too large.

The R 2 clusters (3,2,2) and (3,3,0) were treated similarly, as shown in Fig. 9. The agreement between experiment (a) and theory (b) is considerably better in these two cases, assuming $N_1 = 4$, $N_2 = 2$, $N_4 = 3$, and (independently) $N_5 = 4$. (The possible values of N in these cases are 2, 3, and 4.) We also assumed, for the (3,3,0) cluster, a nonzero triplet decay rate of $\gamma_T^0/\gamma_S^0 = 1.48$ in the computed spectra (*vide infra*). Avoided crossings occur in these clusters at still higher fields[16]; the positions of these are also accurately reproduced by the calculations.

We also examined, experimentally, the magnetic-field dependence of several P-branch transitions. Probable ME's of low intensity associated with P 1 could not be observed because of severe overlap with the Q branch. A small splitting of about 15 MHz was observed for the (1,1,1) component of the P 2 transition at a field of 66 G. The P 3 transition shows a magnetic-field dependence that is similar to the R 1 transition. P 4 also behaves similarly to R 2, but was not analyzed because of the additional complications caused by the presence of strong transitions to the levels (3,1,3) and (3,0,3).

C. Effect of triplet–triplet coupling

In an effort to improve the agreement between theory and experiment, particularly for the R 1 transition, the effects of triplet–triplet coupling on the ME spectra and their field dependence have been considered in some detail. That such coupling might occur is reasonable. Since the fine structure splitting exceeds the typical separation of the different zero-order triplets that interact with the singlet (cf. Fig. 7), these triplets cannot be the fine structure levels of a single vibronic state. Instead, the triplet levels that are involved must belong to *different* vibrational states of the zero-order triplet manifold. Field-independent mixing between these levels, what we have previously called *interrovibronic* mixing,[33] could play a significant role in this problem.

If two or more triplet levels are coupled, the Hamiltonian matrix in the zero-order basis [Eq. (2)] will then contain off-diagonal elements connecting them, rendering the procedure of Lawrance and Knight[32] invalid. However, it is always possible to apply a unitary transformation that removes these elements, thereby prediagonalizing the matrix with respect to *specific* interactions. Applying the deconvolution procedure to this transformed matrix will then produce a set of energies and matrix elements that describe the coupling of the transformed triplet levels to the zero-order singlet state.

As an example, we treat the case of one singlet level $|S^0\rangle$ coupled to two zero-order triplet levels, $|T_1^0\rangle$ and $|T_2^0\rangle$, that are coupled to each other via some field-independent matrix element α. The Hamiltonian has the form

$$\hat{H}_0 = \begin{array}{c} \begin{matrix} |S^0\rangle & |T_1^0\rangle & |T_2^0\rangle \end{matrix} \\ \begin{vmatrix} \epsilon_S^0 & v_1 & v_2 \\ v_1 & \epsilon_{T_1}^0 & \alpha \\ v_2 & \alpha & \epsilon_{T_2}^0 \end{vmatrix} \end{array} . \tag{14}$$

Applying a unitary transformation that removes the off-diagonal term α, we have

$$\hat{H}_0' = \begin{array}{c} \begin{matrix} |S\rangle & |T_1\rangle & |T_2\rangle \end{matrix} \\ \begin{vmatrix} \epsilon_S^0 & v_1' & v_2' \\ v_1' & \epsilon_{T_1} & 0 \\ v_2' & 0 & \epsilon_{T_2} \end{vmatrix} \end{array} . \tag{15}$$

Of course, the eigenvalues and eigenfunctions of this Hamiltonian are the same as those of Eq. (14). But the transformation changes the coupling terms v_1 and v_2 into v_1' and v_2', and converts the zero-order triplet functions into the transformed functions

$$\begin{aligned} |T_1\rangle &= c_1|T_1^0\rangle + c_2|T_2^0\rangle , \\ |T_2\rangle &= -c_2|T_1^0\rangle + c_1|T_2^0\rangle \end{aligned} \tag{16}$$

with $|c_1|^2 + |c_2|^2 = 1$. since Eq. (15) has the same form as Eq. (2), applying the deconvolution procedure to the spectrum yields the relative energies ϵ_S, ϵ_{T_1}, ϵ_{T_2} and coupling terms v_1', v_2', values that are different from those that would be obtained if triplet–triplet coupling did not exist. Thus we conclude that information about such coupling, if it exists, is already contained in the wave functions, energies, and matrix elements derived from applying the deconvolution recipe to the experimental spectra (Table IV).

Consider, now, the case when an external magnetic field is applied. The matrix elements of the isotropic electron spin Zeeman operator $\hat{H}_Z$ acting on the zero-order triplet levels $|T_{1,2}^0\rangle = |v_1,v_2,N_1,N_2,K_1,K_2,S,J,M_J\rangle$ are given by[38]

$$\begin{aligned} \langle T_2^0|\hat{H}_Z|T_1^0\rangle &= \langle v_2N_2K_2SJM_J|\hat{H}_Z|v_1N_1K_1SJM_J\rangle \\ &= \delta(v_2,v_1)\mu_B Bg(J,N_2,N_1,S)M_J . \end{aligned} \tag{17}$$

Here, $\delta(v_2,v_1)$ indicates that the operator is diagonal in all vibrational quantum numbers simultaneously; $g(J,N_2,N_1,S)$ reduces to Eq. (11) if $N_2 = N_1 = N$. The matrix of $\hat{H}_Z$ in the transformed basis is then

$$\hat{H}_Z' = \begin{vmatrix} 0 & 0 & 0 \\ 0 & \langle T_1|\hat{H}_Z|T_1\rangle & \langle T_2|\hat{H}_Z|T_1\rangle \\ 0 & \langle T_1|\hat{H}_Z|T_2\rangle & \langle T_2|\hat{H}_Z|T_2\rangle \end{vmatrix} , \tag{18}$$

where

$$\langle T_1|\hat{H}_Z|T_1\rangle = |c_1|^2\langle T_1^0|\hat{H}_Z|T_1^0\rangle + |c_2|^2\langle T_2^0|\hat{H}_Z|T_2^0\rangle ,$$
$$\langle T_2|\hat{H}_Z|T_2\rangle = |c_2|^2\langle T_1^0|\hat{H}_Z|T_1^0\rangle + |c_1|^2\langle T_2^0|\hat{H}_Z|T_2^0\rangle ,$$
$$\langle T_1|\hat{H}_Z|T_2\rangle = \langle T_2|\hat{H}_Z|T_1\rangle^* = -c_1^*c_2\langle T_1^0|\hat{H}_Z|T_1^0\rangle + c_1c_2^*\langle T_2^0|\hat{H}_Z|T_2^0\rangle . \quad (19)$$

Owing to the orthogonality of the (zero-order) vibrational wave functions, cross terms like $\langle T_1^0|\hat{H}_Z|T_2^0\rangle$ in Eq. (19) vanish since $|T_1^0\rangle$ and $|T_2^0\rangle$ are assumed to belong to different vibrational species. But Eq. (18) shows that the presence of triplet–triplet coupling introduces additional off-diagonal Zeeman terms, and modifies existing diagonal ones, despite the fact that this coupling is field independent. Modifications in the behavior of the calculated ME spectrum in the presence of a field are then expected to occur.

We used the following procedure to examine these effects. First, since the term α coupling $|T_1^0\rangle$ and $|T_2^0\rangle$ is unknown, an extra parameter was introduced into the calculation. We chose this to be the mixing coefficient c_1. (Additional adjustable coefficients would have to be introduced if more than two triplet levels were involved.) Then, the matrix $\hat{H}'_Z$ of Eq. (18) was added to that of Eq. (15), and the sum was diagonalized to find the eigenvalues, eigenvectors, and the ME spectrum in the presence of a field.

Figure 10 shows some typical results. Here we compare the calculated field dependence of the (2,2,1) cluster [Fig. 10(b)] with that observed experimentally [Fig. 10(a)]. As before, $N_1 = 1$ and $N_2 = 3$; the optimum value of c_1 was found to be 0.8, giving the transformed triplet functions

$$|T_1\rangle = 0.8|T_1^0\rangle - 0.6|T_2^0\rangle ,$$
$$|T_2\rangle = 0.6|T_1^0\rangle + 0.8|T_2^0\rangle . \quad (20)$$

The result is a modified Zeeman pattern, caused by a change in the effective g values of the coupled states. In this case, since

$$\langle T_1|\hat{H}_Z|T_1\rangle = |c_1|^2\langle T_1^0|\hat{H}_Z|T_1^0\rangle + |c_2|^2\langle T_2^0|\hat{H}_Z|T_2^0\rangle = |c_1|^2g_1M_J\mu_BB + |c_2|^2g_2M_J\mu_BB = (|c_1|^2g_1 + |c_2|^2g_2)M_J\mu_BB \quad (21)$$

and similarly for $\langle T_2|\hat{H}_Z|T_2\rangle$, we have

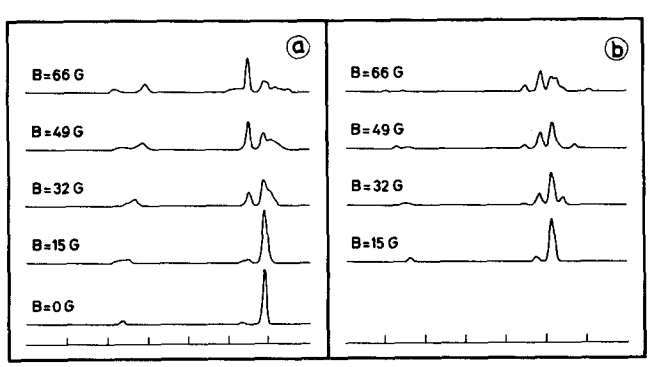

FIG. 10. Comparison of observed (left) and calculated (right) magnetic field dependence of the perturbed (2,2,1) cluster in the R 1 transition. Here, the calculation includes a possible coupling between the triplet levels 1 and 2. The separation between each pair of markers is 100 MHz. Frequency increases from left to right.

$$g_1^{\text{eff}} = |c_1|^2g_1 + |c_2|^2g_2 = 0.40 ,$$
$$g_2^{\text{eff}} = |c_2|^2g_1 + |c_1|^2g_2 = -0.07 , \quad (22)$$

where $g_1 = 1.00$ and $g_2 = -0.67$ in the zero-order representation. While some quantitative difficulties remain, the computed spectrum now shows qualitatively the correct behavior. In particular, line 2 now gains intensity at the expense of line 3, and the splitting pattern of the main group of lines bears a much closer resemblance to experiment.

D. Coupling to a continuum

A logical extension of the above arguments is to assume that the affected triplet levels are coupled to a "continuum," allowing the excited molecule to decay nonradiatively. Such a coupling could be caused by Coriolis interactions or other nonrigid body effects, involving either other triplet states or the ground state. If the jth ME is expanded according to the usual recipe,

$$|\text{ME}_j\rangle = c_S|S^0\rangle + \sum_i c_{T_i}|T_i^0\rangle \quad (23)$$

the decay rate of this state is given by

$$\gamma_{\text{ME}_j} = |c_S|^2\gamma_S^0 + \sum_i |c_{T_i}|^2\gamma_T^0 , \quad (24)$$

where γ_S^0 and γ_T^0 are the zero-order singlet and triplet decay rates. Assuming a linear response to the laser, the steady-state absorption intensity of the jth ME, A_j, is proportional to $|c_S|^2$. The excitation intensity E_j is proportional to $|c_S|^4/\gamma_{\text{ME}_j}$. Therefore,[39]

$$E_j = \beta\left(\frac{A_j^2}{\gamma_{\text{ME}_j}}\right) , \quad (25)$$

where β is a proportionality constant. If γ_T^0 is small compared to γ_S^0, then γ_{ME_j} is proportional to $|c_S|^2$ and $E_j \propto A_j$. On the other hand, if γ_T^0 is of the same order as γ_S^0, then the absorption intensity is no longer proportional to the excitation intensity. In that event, the experimental intensities in the ME spectrum cannot be used in the deconvolution procedure, which requires absorption intensities.

Without either absorption spectra or measured lifetimes for all of the ME's, we treated the absorption intensity of each ME as an adjustable parameter to address this problem. Figure 11 shows the best results obtained when the (2,2,1) cluster is treated in this way. Here, absorption intensities of 15 and 4 were assumed for lines 1 and 2 (corresponding to γ_T^0/γ_S^0 values of 0.58 and 0.05), rather than the measured excitation intensities of 5 and 2. The deconvolution procedure was then applied anew, yielding a new set of zero-order energies, mixing coefficients, and coupling parameters. To this Hamiltonian were added the appropriate Zeeman terms, again assuming $N_1 = 1$ and $N_2 = 3$, and the result was diagonalized. The derived values of the coefficients in the zero-order basis, c_S and c_{T_i}, were then used to define γ_{ME_j} [using Eq. (24)], from which the excitation intensity could be calculated, via Eq. (25). When computed in this way, the theoretical spectrum [Fig. 11(b)] of the (2,2,1) cluster is found

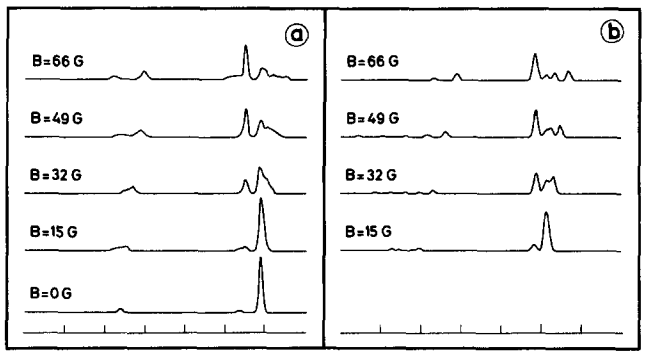

FIG. 11. Comparison of observed (left) and calculated (right) magnetic field dependence of the perturbed (2,2,1) cluster in the R 1 transition. Here, the calculation includes a possible coupling of both triplet levels 1 and 2 to a continuum of dark states. The separation of each pair of markers is 100 MHz. Frequency increases from left to right.

to compare very favorably with that observed experimentally [Fig. 11(A)].

V. DISCUSSION

The spectroscopic results presented in this paper have significant dynamic implications, especially for the radiationless process known as intersystem crossing (ISC). Clearly, this process, in which an initially prepared nonstationary singlet state evolves smoothly into a triplet state, is promoted by perturbed levels that contain both singlet and triplet character. Our experiments have identified some of these levels for the first time. And the results show that the number of perturbed levels in the vicinity of the $^1B_1$ origin is very small, at least for low J',K'. The average triplet character of the bright levels is also small. From this we can conclude that as an isolated species, pyrimidine will behave as a small molecule when excited to the $^1B_1$ origin with a light source of small coherence width. Under these conditions, "reversible" decay is expected and ISC, if it occurs at all, is principally collision induced, as observed in a variety of time-domain experiments.[12–14] The cross section ($\sigma_{\rm ISC}$) for collision-induced ISC depends, in turn, on the triplet state rotational relaxation cross section and on the average triplet character of the prepared state.[40] Since we have seen that this character is increased by the application of a magnetic field, $\sigma_{\rm ISC}$ should also be field dependent, a fact that has also been verified experimentally.[16] Fluorescence quenching by a field should also be very weak, as in other small molecules.

Increasing the coherence width of the light source will modify the decay behavior of the isolated molecule, owing to an increase in the number of coupled states that participate in the excitation process. If this increase is fast enough, the molecule could develop statistical properties after passing through the intermediate case. But the spectroscopic results show that only a limited number of coupled states exist in (say) a few GHz region around the singlet origin. This leads to the prediction that pyrimidine should behave as a (sparse) intermediate case molecule under picosecond excitation conditions. In agreement with this, Saigusa *et al.*[15] observed only quantum beats in the fluorescence decay of the 0_0^0 band following excitation with a few picosecond laser pulse. The observed frequencies of these beats were 60 and 140 MHz. Of course, it is impossible to know which levels were being excited in the experiments of Saigusa *et al.*[15] But the existence of such recurrences on this time scale is certainly consistent with our spectroscopic results, which show that perturbations, and splittings, of this order of magnitude are present in the S_1 manifold. So, in this sense, our results are not at all surprising. We cannot, of course, comment on the apparent transition to an increasingly statistical behavior that has been observed in time-domain experiments at higher energies above the $^1B_1$ origin[15] without further *ultra* high-resolution work.

More important dynamic issues do surface, however, on closer examination of our results, issues that cannot normally be addressed in the time domain. One question of extreme importance is the mechanism by which the zero-order triplet levels gain their radiative character. Clearly, spin–orbit coupling plays a role, and since this coupling probably involves states of similar ($n\pi^*$) character, the matrix elements are expected to be small, as observed. But are there promoting modes and accepting modes, time-honored concepts in the theory of radiationless transitions? What are the relative displacements of the zero-order singlet and triplet surfaces along different normal coordinates? Indeed, is it proper to speak of normal modes at high triplet vibrational energies? And are rotations important, either as a source of additional coupling terms or as a mechanism for mixing vibrational levels? Could axis switching play a role? And what about "smaller" effects, such as hyperfine mixing?

Not all of these issues can be resolved here. But one, that of the possible influence of rotations, can be addressed constructively. There is mounting evidence that rotations are important in *intra*molecular dynamics.[17,41,42] In the case of pyrimidine, Baba *et al.*[43] observed a marked variation in the fluorescence quantum yield across the rotational contour of the 0_0^0 band in the vapor phase at low pressure, with a very steep peak near the band origin. Jameson *et al.*[44] compared the fluorescence decay properties of effusive and jet-cooled samples of pyrimidine, and found an enhanced contribution of the slow component to the biexponential decay of the $0_0^0 + \nu_{6a}$ band at lower temperatures. Saigusa and Lim[45] found that $A_{\rm fast}/A_{\rm slow}$ increased approximately linearly with J' following excitation of the 0_0^0 band with a pulsed laser having a coherence width of $\sim 0.3\ {\rm cm}^{-1}$. Bartles and Spears[46] detected rotational effects in the fluorescence decay properties of pyrimidine. The possible rotational state dependence of IVR in S_1 pyrimidine has been studied by several authors.[47] And fluorescence polarization[48,49] has been used as a probe of the rotational dynamics of the isolated molecule. Ohta *et al.*[50] showed that the polarization P varies considerably across the rotational contour of the 0_0^0 band, peaking at the Q branch. But Nathanson and McClelland[51] found a value $P = 15.5\%$ for the 0_0^0 band at room temperature, close to the regular-rotor limiting value of $P = 14.4\%$. Additional experiments in a supersonic jet showed that the rotational temperature dependence of the polarization is weak. More recently, Terazima and Lim[52] found that the decay of the polarized fluorescence of the 0_0^0 band is faster than the decay of the slow-component emission, but slower than the decay

of the fast component, and argued that this behavior provided evidence for partial K mixing in the triplet manifold. Clearly, then, rotations *are* involved. The question is, how?

To answer this question, we summarize here the relevant spectroscopic results for the lowest rotational states. We find (a) selected perturbations in the *ultra* high-resolution spectrum of the 0_0^0 band. The most perturbed levels are those with $J' = K'_{-1}$, $K'_{+1} = 1$, which exhibit shifts on the order of 100 MHz. We also find (b) a K'_{+1} dependence of the fluorescence lifetimes, with higher K'_{+1} levels typically exhibiting longer lifetimes (cf. Table I). This is illustrated more clearly in Fig. 12 which shows that the measured lifetimes of levels with the same K'_{+1} and different J' scale approximately linearly with K'_{+1}. The quantitative relationship is

$$\tau = (584 + 80K'_{+1})\ \text{ns}. \tag{26}$$

It is important to note, at this juncture, that the measured lifetimes of *all* levels are longer than the reciprocal spectral resolution (500 ns $\sim$ 1/0.3 MHz). An analysis of the spectral perturbations using standard deconvolution procedures shows that (c) the magnitudes of the off-diagonal elements in the zero-order basis are small and (d) that, as a result, the *calculated* shifts in the spectral lines from their zero-order positions are small, typically less than those observed experimentally. There is no evidence for a J',K' dependence of the number of coupled states or the average triplet character of a "prepared" state from the deperturbation results. Finally, in our attempts to simulate the magnetic-field dependence of the *ultra* high-resolution spectra, (e) improved agreement between experiment and theory is obtained when it assumed that the zero-order triplets are also coupled amongst themselves, either discretely or to a continuum of other triplet or ground state levels. The effect of such coupling, if it exists, is already contained in the matrix elements derived by deconvoluting the spectra.

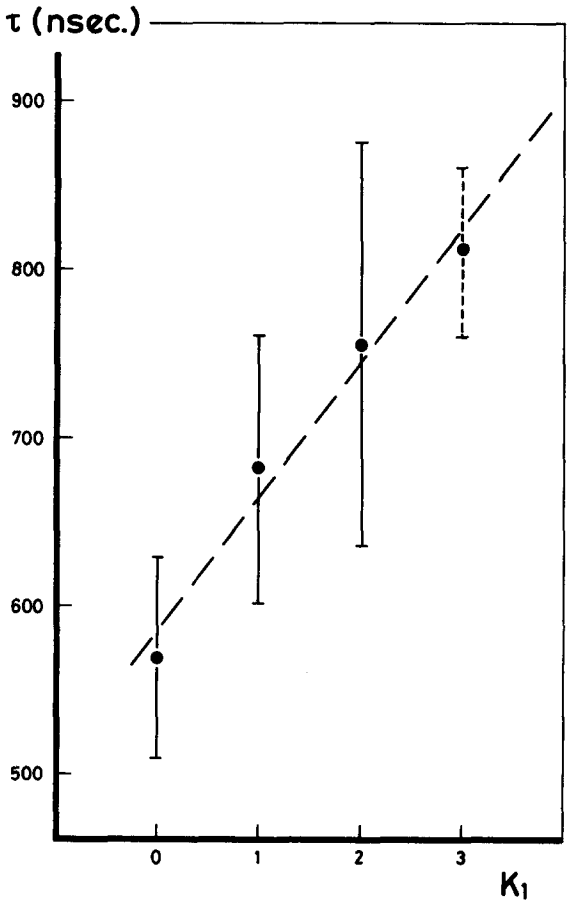

FIG. 12. Plot of the measured fluorescence lifetimes, averaged over J', as a function of the K'_{+1} value of the upper state.

The only logical conclusion to be derived from these results is that the decay behavior of the isolated molecule is dependent on rotational state (Fig. 12), the observed K'_{+1} dependence being consistent with a parallel Coriolis coupling scheme.[53] Whether this coupling involves zero-order triplets or ground state levels is not clear. But the magnitudes of the Coriolis matrix elements must be small, smaller than are observable at the present level of spectral resolution. The broadened dark background states that participate in this process are obscured by the Doppler width of the lines, and make their appearance only indirectly. The reduced values of g^{eff} required to fit the spectra provide one such indicator. But, as in the case of the "Channel Three" region of C_6H_6,[11] we would also expect some K' (or J') dependence of the homogeneous linewidths in the pyrimidine spectra, and of the matrix elements. From the lifetime measurements, it is clear that these dependences will make their appearance directly only when the resolution of the frequency-domain experiment is increased by 1–2 orders of magnitude. The dynamics of S_1 pyrimidine is very slow compared to that of the 14^11^2 S_1 vibrational state of benzene!

The spectroscopic data obtained to date for pyrimidine thus support the following picture of ISC in the isolated molecule. At energies near the $^1B_1$ origin, $\sim$2000 cm^{-1} above the $^3B_1$ origin, the density of triplet rovibronic levels is low, about 10/cm^{-1}. Singlet rovibronic levels, the sources of oscillator strength, are therefore imbedded in a relatively sparse manifold of dark triplet rovibronic levels, and a much higher density manifold of dark ground state levels. The extent to which a given singlet level is coupled with this bath of nonradiative states depends on their level density, of course, but also depends on the rotational angular momentum quantum number K'_{+1} of the prepared state. This is because J' is conserved, at zero field, and because the extent to which a given, strongly coupled zero-order triplet level is coupled with other triplet or ground state levels also depends, through Coriolis coupling, on K'_{+1}. Thus, in the R 1 cluster, component 1 is "strongly" spin–orbit coupled to component 3 and component 2 is only weakly coupled (Table IV). Component 2 gains its oscillator strength by Coriolis coupling with component 1 which is, in turn, strongly coupled to component 3. It is the near-zero energy denominator of the 2/3 coupling that makes this indirect coupling scheme so efficient as a source of energy flow in the isolated molecule. A similar model accounts for the known dynamics of ISC in pyrazine.[17]

We are intrigued by some parallels between this situation and the concepts of resonances and antiresonances in semiclassical dynamics.[54,55] States 1 and 3 in the R 1 cluster are like a resonance, providing direct access to the vibration-

al phase space of the state represented by 1. State 2, like an antiresonance, is only weakly and indirectly coupled to state 3, a coupling that is a strong function of rotational motion. "Turning-on" such motion thereby provides access to another part of vibrational phase space, represented by 2. This coupling is what is responsible for rotational effects in intramolecular dynamics.

ACKNOWLEDGMENTS

We thank Dr. W. Ubachs and Mr. P. Uijt de Haag for experimental assistance, Dr. W. M. van Herpen for helpful discussions, and Professor Dr. A. Dymanus and Professor Dr. J. Kommandew for stimulating interest. This work has been supported by NATO, the U. S. National Science Foundation (INT-84101313, CHE-8402996, and CHE-8419386), and the Nederlandse Organisatie voor Zuiver-Wetenschappelijk Onderzoek (ZWO).

[1]B. J. van der Meer, H. Th. Jonkman, J. Kommandeur, W. L. Meerts, and W. A. Majewski, Chem. Phys. Lett. **92**, 565 (1982).
[2]H. L. Dai, C. L. Korpa, J. L. Kinsey, and R. W. Field, J. Chem. Phys. **82**, 1688 (1985).
[3]J. Bordé, Ch. J. Bordé, C. Salomon, A. van Lerberghe, M. Ouhayoun, and C. D. Cantrell, Phys. Rev. Lett. **45**, 14 (1980).
[4]K. Fox, H. W. Galbraith, B. J. Krohn, and J. D. Louck, Phys. Rev. A **15**, 1363 (1977).
[5]W. A. Majewski, Opt. Commun. **45**, 201 (1983).
[6]A preliminary communication of these results may be found in W. L. Meerts and W. A. Majewski, Laser Chem. **5**, 339 (1986).
[7]A. R. W. McKellar, P. R. Bunker, T. J. Sears, K. M. Evenson, R. J. Saykally, and S. R. Langhoff, J. Chem. Phys. **79**, 5251 (1983).
[8]H. Petek, D. J. Nesbitt, D. C. Darwin, and C. B. Moore, J. Chem. Phys. **86**, 1172 (1987); H. Petek, D. J. Nesbitt, C. B. Moore, F. W. Birss, and D. A. Ramsay, *ibid.* **86**, 1189 (1987).
[9]R. Kullmer and W. Demtröder, J. Chem. Phys. **83**, 2712 (1985).
[10]P. Dupre, R. Jost, and M. Lombardi, Chem. Phys. **91**, 355 (1984).
[11]U. Schubert, E. Riedle, H. J. Neusser, and E. W. Schlag, J. Chem. Phys. **84**, 6182 (1986).
[12]K. G. Spears and M. El-Manguch, Chem. Phys. **24**, 65 (1977).
[13]H. Baba, N. Ohta, O. Sekiguchi, M. Fujita, and K. Uchida, J. Phys. Chem. **87**, 973 (1983).
[14]A. E. W. Knight, J. T. Jones, and C. S. Parmenter, J. Phys. Chem. **87**, 973 (1983).
[15]H. Saigusa, A. K. Jameson, and E. C. Lim, J. Chem. Phys. **79**, 5228 (1983).
[16]Y. Matsumoto and D. W. Pratt, J. Chem. Phys. **81**, 573 (1984).
[17]For a recent review of work on pyrazine, see J. Kommandeur, W. A. Majewski, W. L. Meerts, and D. W. Pratt, Annu. Rev. Phys. Chem. **38**, 433 (1987).
[18]W. A. Majewski and W. L. Meerts, J. Mol. Spectrosc. **104**, 271 (1984).
[19]S. Gerstenkorn and P. Luc, *Atlas du Spectroscopie d'absorption d'iodide* (CNRS, Paris, 1978).
[20]K. K. Innes, H. D. McSwiney, J. D. Simmons, and S. G. Tilford, J. Mol. Spectrosc. **31**, 76 (1969).
[21]J. T. Hougen and J. K. G. Watson, Can. J. Phys. **43**, 298 (1965).
[22]S. W. Thakur and K. K. Innes, J. Mol. Spectrosc. **52**, 130 (1974).
[23]R. E. Smalley, L. Wharton, D. H. Levy, and D. W. Chandler, J. Mol. Spectrosc. **66**, 375 (1977).
[24]G. Herzberg, *Electronic Spectra of Polyatomic Molecules* (Van Nostrand, New York, 1966).
[25]G. L. Blackman, R. D. Brown, and F. R. Burden, J. Mol. Spectrosc. **35**, 444 (1970).
[26]A. Weber, J. Chem. Phys. **73**, 3952 (1980).
[27]D. W. Pratt and H. P. Broida, J. Chem. Phys. **50**, 2181 (1969), and references therein.
[28]H. Lefebvre-Brion and R. W. Field, *Perturbations in the Spectra of Diatomic Molecules* (Academic, New York, 1986).
[29]J. K. G. Watson, J. Chem. Phys. **46**, 1935 (1967).
[30]C. L. Talcott and R. J. Myers, Mol. Phys. **12**, 549 (1967).
[31]A. E. W. Knight, C. M. Lawburgh, and C. S. Parmenter, J. Chem. Phys. **63**, 4336 (1975).
[32]W. D. Lawrance and A. E. W. Knight, J. Phys. Chem. **89**, 917 (1985).
[33]Y. Matsumoto, L. H. Spangler, and D. W. Pratt, J. Chem. Phys. **80**, 5539 (1984).
[34]D. M. Burland and J. Schmidt, Mol. Phys. **22**, 19 (1971).
[35]I. C. Bowater, J. M. Brown, and A. Carrington, Proc. R. Soc. London Ser. A **333**, 265 (1973).
[36]W. Gordy and R. L. Cook, *Microwave Molecular Spectra* (Interscience, New York, 1970).
[37]N. Ohta, M. Fujita, and H. Baba, Chem. Phys. Lett. **135**, 330 (1987).
[38]J. M. Brown and T. J. Sears, Mol. Phys. **34**, 1595 (1977).
[39]W. M. van Herpen, W. L. Meerts, K. E. Drabe, and J. Kommandeur, J. Chem. Phys. **86**, 4396 (1987).
[40]W. M. Gelbart and K. F. Freed, Chem. Phys. Lett. **18**, 470 (1973).
[41]E. Riedle, H. J. Neusser, and E. W. Schlag, J. Phys. Chem. **86**, 4847 (1982); E. Riedle and H. J. Neusser, J. Chem. Phys. **80**, 4686 (1984).
[42]A. Amirav, J. Jortner, M. Terazima, and E. C. Lim, Chem. Phys. Lett. **133**, 179 (1987).
[43]H. Baba, M. Fujita, and K. Uchida, Chem. Phys. Lett. **73**, 425 (1980).
[44]A. K. Jameson, S. Okajima, and E. C. Lim, J. Chem. Phys. **75**, 480 (1981).
[45]H. Saigusa and E. C. Lim, Chem. Phys. Lett. **88**, 455 (1982); J. Chem. Phys. **78**, 91 (1983).
[46]D. M. Bartels and K. G. Spears, J. Phys. Chem. **86**, 5180 (1982).
[47]H. Saigusa, B. E. Forch, and E. C. Lim, J. Chem. Phys. **78**, 2795 (1983); B. E. Forch, K. T. Chen, H. Saigusa, and E. C. Lim, J. Phys. Chem. **87**, 2280 (1983); B. E. Forch and E. C. Lim, Chem. Phys. Lett. **110**, 593 (1984).
[48]Y. Matsumoto, L. H. Spangler, and D. W. Pratt, Chem. Phys. Lett. **95**, 343 (1983).
[49]G. M. Nathanson and G. M. McClelland, J. Chem. Phys. **81**, 629 (1984).
[50]N. Ohta, O. Sekiguchi, and H. Baba, J. Chem. Phys. **82**, 1609 (1985).
[51]G. M. Nathanson and G. M. McClelland, J. Chem. Phys. **84**, 3170 (1986).
[52]M. Terazima and E. C. Lim, J. Chem. Phys. **86**, 8 (1987).
[53]E. B. Wilson, J. Chem. Phys. **4**, 313 (1936).
[54]M. J. Davis, J. Chem. Phys. **83**, 1016 (1985).
[55]C. C. Martens, M. J. Davis, and G. S. Ezra, Chem. Phys. Lett. **142**, 519 (1987).